Thematic set:
Geological storage of CO_2, gas and energy

PG
Petroleum Geoscience

Published online April 27, 2017

https://doi.org/10.1144/petgeo2016-049 | Vol. 23 | 2017 | pp. 306–314

Compressed air energy storage in porous formations: a feasibility and deliverability study

Bo Wang* **& Sebastian Bauer**

Institute of Geosciences, University of Kiel, Kiel, Germany
B.W., 0000-0001-5721-0007
* Correspondence: bo.wang@gpi.uni-kiel.de

Abstract: Compressed air energy storage (CAES) in porous formations is considered as one option for large-scale energy storage to compensate for fluctuations from renewable energy production. To analyse the feasibility of such a CAES application and the deliverability of an underground porous formation, a hypothetical CAES scenario using an anticline structure is investigated. Two daily extraction cycles of 6 h each are assumed, complementing high solar energy production around noon. A gas turbine producing 321 MW of power with a minimum inlet pressure of 43 bar at 417 kg s^{-1} air is assumed. Simulation results show that using six wells the 20 m-thick storage formation with a permeability of 1000 mD can support the required 6 h continuous power output of 321 MW, even reaching 8 h maximally. For the first 30 min, maximum power output is higher, at 458 MW, continuously dropping afterwards. A sensitivity analysis shows that the number of wells required does not linearly decrease with increasing permeability of the storage formation due to well inference during air extraction. For each additional well, the continuous power output increases by 4.8 h and the maximum power output within the first 30 min by 76 MW.

Received 31 March 2016; **revised** 22 March 2017; **accepted** 28 March 2017

The transition of the energy supply from carbon-rich fossil fuels to renewable energy sources, termed the ‘Energiewende’ in Germany, is pursued by many countries in the world as a means of reducing greenhouse gas emission and mitigating climate change effects (Morris & Pehnt 2012; IPCC 2014). For example, in 2014, the share of renewable energy in Germany’s energy supply reached 27.8% and prospectively increases to 40 – 45% in 2025 (BMWi 2015), and may even reach 100% by 2050 (Klaus *et al*. 2010). In the European Union (EU), the share of energy from renewable sources in the gross final consumption of energy reached 15.3% by 2014 and promisingly accomplishes the final target of 20% by 2020 (European Commission 2015). Major renewable energy sources are electric power generation by wind or solar power plants, which causes strong temporal fluctuations of the generated power due to the short-term weather conditions. The possible solutions, such as grid-scale storage systems, improvement of cross-border grid connectivity and electrical demand-side management, can be used to compensate these fluctuations (Sterner & Stadler 2014). Owing to the insufficiency in power transmission lines (Bundesnetzagentur 2015; MELUR 2015), a large amount of construction work is required to improve the current cross-border grid connectivity. Energy demand fluctuates on frequencies varying from less than hourly over daily to seasonally, which introduces more difficulties in managing fluctuating renewable energy production to match the instantaneous energy demand (Kabuth *et al.* 2017). Grid-scale standby storage systems, however, are more flexible in terms of different timescales. In order to stabilize the power grid and meet the demand during times of low renewable power production, a storage demand for Germany of up to 50 TWh electrical energy by 2050 may be required (Klaus *et al.* 2010). Besides pumped hydro-storage as the main large-scale above-ground storage option (Sterner & Stadler 2014), subsurface geological storage has the largest potential to provide such large storage capacities on the longer timescales required (Bauer *et al.* 2013). Storage options include underground storage of natural gas (e.g. Bary *et al.* 2002), which accounts for about 20% of yearly demand in Germany in both salt cavern and porous formation storage facilities (LBEG 2015), underground storage of hydrogen produced from surplus electric power via electrolysis (Pfeiffer & Bauer 2015; Reitenbach *et al.* 2015; Pfeiffer *et al.* 2016, 2017), compressed air energy storage (Crotogino *et al.* 2001) or subsurface storage of heat (Boockmeyer & Bauer 2016; Popp *et al.* 2016).

Compressed air energy storage (CAES) is seen as a promising option for balancing short-term diurnal fluctuations from renewable energy production, as it can ramp output quickly and provide efficient part-load operation (Succar & Williams 2008). CAES is a power-to-power energy storage option, which converts electricity to mechanical energy and stores it in the subsurface (Sternberg & Bardow 2015). For CAES, off-peak energy is used to store energy as highly compressed air, which is used to generate power through gas turbines during times of peak demand. Subsurface storage of compressed air in salt caverns or porous formations offers large storage capacities. Currently, only two CAES facilities (i.e. in Huntorf in Germany and in McIntosh, Alabama, USA) are operating, both using subsurface salt caverns as reservoir for the compressed air (Raju & Khaitan 2012). Salt caverns can be mined at different depths within a suitable salt dome (Kepplinger *et al.* 2011), which allows for a range of operation pressures. There is no inherent limitation on the deliverable air flow rates, like the hydraulic permeability in porous formations (Kushnir *et al.* 2012*b*). This can allow better control of reservoir conditions with the use of salt caverns compared to porous formations. Nonetheless, porous formations have a much wider geological availability compared to rock salt suitable for caverns and may provide much larger storage capacities (Kabuth *et al.* 2017). Furthermore, the storage capacity of a porous formation can be extended by injecting additional air to develop a larger gas reservoir, or by drilling additional wells. However, increasing the cavern size also increases the risk of instability (Succar & Williams 2008), so that additional caverns have to be constructed if storage size is increased. The first study of CAES using a porous formation was conducted in Pittsfield, Illinois, USA, and showed that the concept is feasible at this site (ANR Storage Company 1990). A review by Succar & Williams (2008) comprehensively described the technical and economic possibilities of large-scale CAES storage sites with wind farms, and also addressed the possibilities when using a porous formation as a CAES storage reservoir. However, a planned CAES facility in a porous formation in Iowa, USA was stopped due to inadequate local geological conditions, as well as energy market reasons (Schulte *et al.* 2012).

So far, research has focused on studying the feasibility of CAES using salt caverns as storage reservoirs to investigate hydraulic, thermal and mechanical behaviours during operation (Heusermann *et al.* 2003; Kushnir *et al.* 2012*b*; Nazary Moghadam *et al.* 2013; Khaledi *et al.* 2016*a*, *b*), as well as on CAES technology developments yielding optimized CAES plant configurations with enhanced efficiency (Nakhamkin *et al.* 2009; Ibrahim *et al.* 2010; Hartmann *et al.* 2012; Luo *et al.* 2016). Regarding underground CAES in porous formations, Kushnir *et al.* (2010) performed a simplified analytical investigation of a compressible gas flow within CAES porous formation storage reservoirs to calculate, for example, the optimal critical air flow rate for different formation thicknesses, well screen lengths and diameters. Pei *et al.* (2015) analysed the performance of a CAES plant for different permeabilities of the storage formation by analytical thermodynamic calculations, and stated that both thermal and exergy efficiencies increase with increasing permeability. Oldenburg & Pan (2013*a*, *b*) simulated an idealized gently domed CAES porous formation storage site and proved the feasibility of CAES operation using a single wellbore. None of the reported studies represents a large-scale CAES application in a porous formation or accounts for a representative geological setting of the storage formation.

Therefore, this study investigates the feasibility of operating a large-scale CAES plant with a geometrically representative porous formation storage site by estimating the deliverability of the storage formation, as well as the potential capacity. To reach this aim, a porous formation in a geological anticline structure was used, which is a representative anticline site from the North German Basin, and a power plant analogous to the Huntorf power plant was assumed. The formation deliverability and the corresponding power output of the CAES plant were determined for different operating conditions, and a sensitivity analysis of the formation permeability and the number of wells required was conducted.

A CAES scenario in a porous formation

The Huntorf power plant is the first commercial CAES facility in the world; it started operating in 1978 and produces 321 MW power of electrical energy maximally for 3 h since an upgrade in 2006 (E.ON SE 2016). The power plant is connected via two wells to the salt storage caverns (Crotogino *et al.* 2001). In this scenario, the same gas turbine set-up is used as for the Huntorf power plant, but, instead of salt caverns, a porous formation is used as the storage reservoir. A schematic sketch of this hypothetical CAES facility is shown in Figure 1. The power plant consists of a compressor, a motor/generator and a gas turbine (Hoffeins 1994). When surplus power from renewable resources is available, the motor drives the compressor to compress air, which is then stored in the subsurface porous formation. During peak demand, the compressed air is released via the wells from the formation and burned with natural gas at a rate of 11 kg s^{-1} in the gas turbine to drive the generator and produce electricity (Hoffeins & Mohmeyer 1986).

The hypothetical CAES facility considered in this work is a conventional diabatic CAES, which stores the energy as highly pressurized air but not the heat from compression. For this kind of CAES power plant, the air mass flow rate and the minimum inlet pressure at the turbine are the most critical design parameters for achieving the targeted power output (Hydrodynamics Group LCC 2011). The Huntorf gas turbine requires an air mass flow rate of 417 kg s^{-1} with a minimum turbine inlet pressure of 43 bar to produce 321 MW of power (Hoffeins 1994; Crotogino *et al.* 2001; Kushnir *et al.* 2012*a*). In addition to energy analysis, exergy is often used to quantify the potential useful work of gas turbines at two specified states (e.g. inlet and outlet) (Çengel & Boles 2011). Under the assumption of a constant air temperature at the turbine inlet, the exergy flow can be roughly estimated from the air mass flow rate and minimum inlet pressure, which represent the potential work done by the compressed air without adding natural gas (Kim *et al.* 2012). For the Huntorf gas turbine, the exergy flow is thus 134 MW, and this is about 42% of the actual power output (Kim *et al.* 2011).

A suitable geological site for compressed air energy storage is given by a highly permeable porous formation and a tight cap rock to prevent the buoyant rise of the air (see Fig. 1). In northern Germany, anticline structures suitable for CAES can be found in a variety of settings (Baldschuhn *et al.* 2001). The tops of anticlines vary from a depth of about 500 to 1500 m, a dip angle from about 8° to 34°, an anticline drop from about 480 to 1400 m and a closure radius from about 1200 to 8000 m. Based on this set of geological data, a synthetic anticline was generated for this work. The anticline top was assumed to be at a depth of 700 m, the drop to be 900 m, a closure radius of roughly 3 km and thus a dip angle of roughly 16° (see Fig. 2). The modelled area containing the anticline covered an area of 16 × 16 km and the storage formation was formed by a 20 m-thick saline formation, bounded by two 30 m-thick water-saturated, but impermeable, layers at the top (cap rock) and bottom. The parameters of this storage formation (Table 1) (e.g. permeability and porosity) refer to on-site data from the Rhaetian sandstone formation in northern Germany given in Hese (2011, 2012) and the statistical study from Dethlefsen *et al.* (2014). This sandstone formation has been investigated for CO_2-sequestration purposes (Hese 2011) and considered for underground hydrogen storage (Pfeiffer *et al.* 2016, 2017). Although the anticline applied here is synthetically generated, its geometrical dimensions and parameters represent a typical anticline structure with a sandstone formation in northern Germany. Open hydraulic boundary conditions are assumed, which allow for brine outflow and pressure relief. However, if pressure relief is too large, no longer-term pressurization due to air injection can be achieved, which would be unfavourable for extracting the air at high flow rates (Oldenburg & Pan 2013*a*).

Compressed air was injected and extracted using a varying number of vertical wells with a 20 inch production string and fibreglass-reinforced plastic as the inner material. Pressure loss was estimated under the assumption that no water phase is present in the extracted air (following Hagoort 1988), and the friction factor was estimated with reference to Goudar & Sonnad (2008). In order to maintain an air pressure of 43 bar at the well head and the turbine inlet, a minimum well bottom hole pressure (BHP) of 47 bar had to be exceeded.

Morris & Pehnt (2012) found that power generation from photovoltaics has grown considerably in recent years, and thus using a daily operation cycle for the hypothetical CAES power plant assumes that surplus energy from photovoltaics is highest at around noon. As shown in Figure 3, the CAES power plant was used to produce power for 6 h in the morning and again in the afternoon, and times of no production were used to inject air and thus recharge the storage. To compensate for the pressure loss due to the open boundaries, the injection air mass flow rate was set to 430 kg s^{-1}, which is slightly larger than the extraction rate of 417 kg s^{-1}.

Simulation set-up

The numerical simulations were performed using the oil and gas reservoir simulator ECLIPSE 300 in compositional mode (Schlumberger 2016), in which compressed air was considered as a compositional gas of 78% N_2, 21% O_2 and 1% Ar. Only the storage formation of the geological anticline was simulated, as the cap rock and bottom rock layers were assumed to be impermeable.

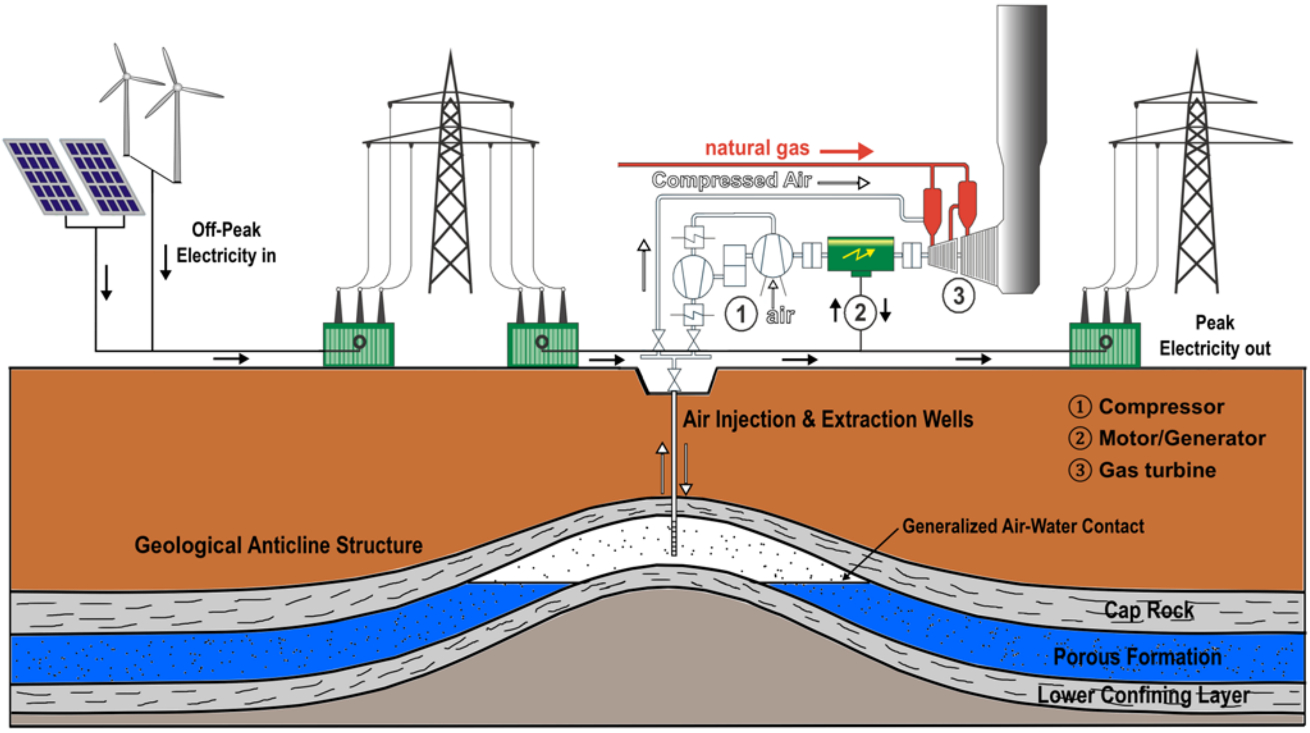

Fig. 1. A schematic sketch of a hypothetical conventional CAES facility using a porous formation as the storage reservoir (modified from Crotogino *et al.* 2001).

The storage formation represents a homogeneous sandstone reservoir of 20 m thickness with a high permeability of 1000 mD, and the corresponding parameters are listed in Table 1. The capillary pressure-saturation function of the reservoir was determined by the Brooks & Corey (1964) correlation. Using compositional gas parameters listed in Table 2, air properties were calculated using a generalized form of the Peng–Robinson equations of state (Schlumberger 2016) in simulations. The gas flow close to wells was simulated as laminar flow, not accounting for the effects of non-Darcy flow, which might in our case slightly lower extraction rates. The storage formation was discretized into $120 \times 120 \times 25$ cells, with a finer horizontal discretization of 10 m around the wells and a coarser discretization of 1000 m at the model boundary. The vertical discretization was gradually coarsened, with finer cells of 0.5 m thickness at the top and coarser cells of 1 m thickness at the bottom.

Initially, the pressure distribution is hydrostatic with 71.95 bar at 720 m depth (Fig. 4a), and the gas–water contact is set to 800 m (Fig. 4b), representing a vertically equilibrated gas phase in the reservoir. This initial condition avoids the explicit simulation of the storage initialization and thus simulations start with the storage gas already in place. The initial gas phase has a radius of roughly 500 m and 3.36×10^8 kg of air in place, which is about 37 times the cyclic amount and enough to maintain the gas–water contact during cyclic operation. With a minimum distance of 200 m between each pair of wells, a total of 21 wells can be placed within that 500 m radius gas reservoir, and the spatial well set-up is shown in Figure 4. All the wells are fully screened wells in the storage formation. With preliminary tests to support our operational schedule, six wells at locations UL, ML, DL, UR, MR and DR (cf. Fig. 4) were required.

As the aquifer of the storage formation is not closed laterally, the lateral boundaries of the simulation model were simulated as open boundaries by using large pore volume cells at the outermost cells of the simulation model, which maintain the hydrostatic pressure initialized in the model. The top and bottom model boundaries were set as closed boundary conditions. The total injection and extraction air mass flow rates of 430 kg s^{-1} and 417 kg s^{-1} were distributed to the six wells. Work by Mitiku & Bauer (2013) shows that the assumption of vertical wells in simulating anticline usage is valid, as only slightly higher rates may be obtained using horizontal drilling techniques. A threshold pressure of 47 bar was set to each well bottom hole during extraction to ensure the minimum gas turbine inlet pressure. In addition, to avoid possible induced fractures in the reservoir rock during injection (e.g. Benisch & Bauer 2013; Mitiku & Bauer 2013), a maximum pressure of 150% of the initial hydrostatic pressure at each well bottom hole (i.e. 108 bar) was applied.

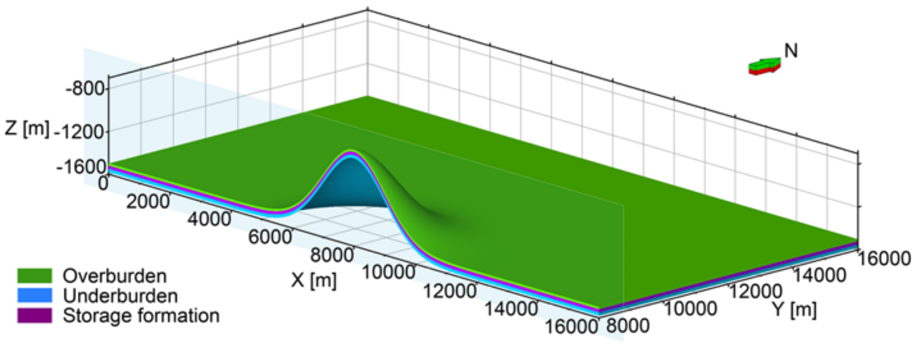

Fig. 2. A synthetic but typical anticline structure used as a storage site (side view). The overburden forms the tight cap rock.

Table 1. *The parameters of the storage formation*

Parameter	Storage formation
Permeability	1000 mD
Porosity	0.35
Residual gas saturation	0.10
Residual water saturation	0.20
Brooks & Corey (1964) λ, P_d	2.5, 0.1 bar
Geothermal gradient	25°C km^{-1}
Water density	1050 kg m^{-3}
Rock density	2650 kg m^{-3}
Water compressibility	4.50×10^{-5} bar^{-1}
Rock compressibility	4.50×10^{-5} bar^{-1}

Feasibility and deliverability analysis

The feasibility study for a large-scale CAES plant needs to validate whether the chosen storage formation can deliver the required air mass flow rate and, at the same time, maintain the pressure response within the given pressure thresholds of the fracture pressure and minimum operation pressure required (Schulte *et al.* 2012). An initial fill of the porous formation is required to form a gas phase, from which the air can be injected and extracted during cyclic operation. This initial fill raises the reservoir pressure above the hydrostatic pressure. However, over time, the pressure in the storage formation dissipates and returns to the initial hydrostatic value, regardless of the cyclic operation, if the storage formation has an open boundary (Benisch & Bauer 2013; Pfeiffer *et al.* 2017). Therefore, the initial hydrostatic pressure is used here to represent the reservoir pressure. This represents the lower limit for the average reservoir pressure during the storage operation, and actually reduces storage deliverability, as some elevated formation pressure would allow for higher extraction rates.

The BHP of six wells during the cyclic operation is shown in Figure 5a. Pressure fluctuates around the initial hydrostatic pressure, and its responses are lower than the maximum safe operation pressure and higher than the minimum required BHP. All wells show the same pressure response and thus the same behaviour, independent of their location in the gas phase. The lowest observed BHP during extraction was 48.2 bar, which is above the 47 bar required by the turbine, and during injection the BHP reaches up to only 89.7 bar maximally, which is well below the 108 bar assumed for fracture pressure. The injection and extraction rates specified thus can be supported by the formation if six wells are used. This indicates that the porous formation simulated can support the cyclic operation of the Huntorf gas turbine, and can sustain a continuous power output of 321 MW for 6 h at an extraction air mass flow rate of 417 kg s^{-1}, corresponding to 1926 MWh of electrical energy production.

Based on the CAES scenario in this study, a deliverability analysis was conducted on the chosen porous formation to investigate the possible energy output (Fig. 5b). First, without refilling the air, the compressed air was continuously extracted from the reservoir by maintaining an extraction air mass flow rate, i.e. gas production rate (GPR), of 417 kg s^{-1} and a well BHP of 47 bar. After 8 h, the extraction air mass flow rate of the six wells started to decrease and the power output dropped (Fig. 5b, 'Defined scenario' and 'Fixed BHP and GPR' lines). This shows that the reservoir can continuously produce 321 MW of power for up to 8 h, delivering a total air mass of 1.2×10^7 kg, which corresponds to 3.5% of the initial air mass. In total, the produced electrical energy was 2568 MWh. After 8 h, the extractable air mass flow rate decreased continuously and, correspondingly, the power output also decreased.

According to the operational experiences of the Huntorf power plant (Hoffeins & Mohmeyer 1986), on some of the working days, the CAES facility needed to start up and reach its full capacity within 30 min due to unexpected failures in the electrical grid. These situations are typical now, as the intermittent energy production from renewable resources leads to an increase in load-balancing requirements. Therefore, the reservoir deliverability and corresponding power output were also investigated for shorter time periods. An estimation of the maximum possible instantaneous power output was performed by only maintaining the well BHP (Fig. 5b, 'Fixed BHP' line) and allowing higher flow rates at the wells. This corresponds to the case where a maximum amount of air is extracted at each point in time and thus instantaneous power is high. In the first 30 min, the average maximum extraction air mass flow rate of the six wells was 596 kg s^{-1}, corresponding to 458 MW of power. The achievable air mass flow rate (Fig. 5b, 'Fixed BHP' line) dropped continuously with time, as air was extracted from the closer vicinity of the wells, and therefore the instantaneous power output also decreases. Based on the instantaneous power, the possible average power output over time was calculated (Fig. 5b, 'Average power' line). It showed, for instance, that after 12 h the actual instantaneous power was 293 MW at an air mass flow rate of 381 kg s^{-1}, while the average power output achieved (i.e. the average output for the 12 h) was 340 MW.

Results of the instantaneous power output show that at 7.5 h the power production was 321 MW. However, according to the continuous power production, the reservoir can produce the same amount of power up to 8 h. This difference is due to the fact that the reservoir was operated at lower extraction rates in the case of a continuous output and the corresponding power could be obtained for longer periods. Thus, the 'Fixed BHP' line in Figure 5b allows for a conservative estimate of the production rates, the corresponding power achieved and the time periods over which the power was provided, so that other shorter operation cycles can also be designed using this line. This provides flexibility in power output as well as in power delivery times, both of which are required for an electricity production dominated by fluctuating renewable energy.

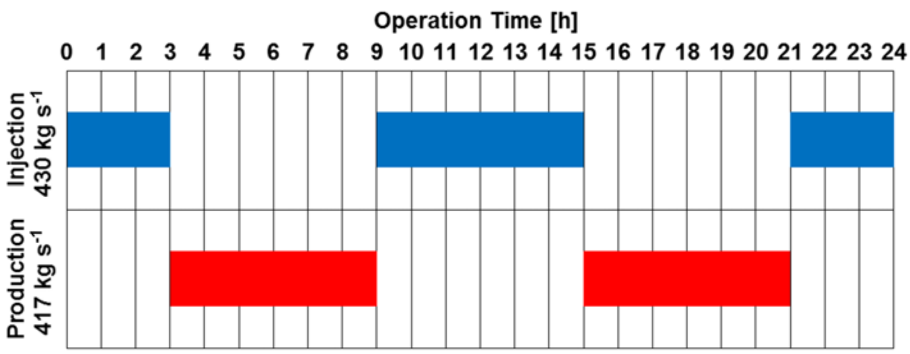

Fig. 3. The daily operation cycle.

Table 2. *The parameters of the air components (Lemmon et al. 2000; Kaye & Laby 2016)*

Parameter	N_2	O_2	Ar
Critical temperature	126.192 K	154.581 K	150.687 K
Critical pressure	33.95 bar	50.43 bar	48.63 bar
Critical molar volume	8.95×10^{-5} m^3 mol^{-1}	7.34×10^{-5} m^3 mol^{-1}	7.46×10^{-5} m^3 mol^{-1}
Acentric factor	0.037	0.022	−0.002

Sensitivity analysis

The permeability of the storage formation strongly affects the deliverability and the power output of an underground CAES storage. To improve the deliverability of a low-permeability formation, one of the approaches is to increase the number of wells used for injecting and extracting the compressed air. However, the investment of drilling wells is very expensive, so it is interesting to investigate the number of wells required for different reservoir conditions and thus design a cost-effective plant. The average permeability of the storage formation was varied from 10 to 2500 mD, and the corresponding porosity varied from 0.15 to 0.40 (see Table 3). The ranges of permeability and porosity used here refer to the on-site data of the Rhaetian formation from the North German Basin given in Hese (2011, 2012) and the statistical study from Dethlefsen *et al.* (2014). As there is no correlation between permeability and porosity reported in this work, an increase in porosity with permeability was assumed, covering the porosity values reported. For different permeabilities of the storage formation, the number of wells needed to support the required flow rate of 417 kg s^{-1} for 6 h is shown in Figure 6. When the permeability was less than 300 mD, even using 21 wells, the storage formation could not support the required air mass flow rate of 417 kg s^{-1} for 6 h: that is, the CAES facility cannot produce 321 MW of power for 6 h. With increasing permeability, fewer wells are required to achieve the specified flow rate. A minimum of three wells is always required, even for a high permeability of 2500 mD. As can be seen in Figure 6, the number of wells required to support the required flow rate does not linearly decrease with increasing permeability of the storage formation. This is due to well interference occurring at longer extraction times, and it causes higher well numbers compared to the case of no well interference.

In addition, we carried out a study to estimate the power output of the designed CAES scenario if different numbers of wells were used, and investigated the efficiency of the power output increase achieved from only using more wells. The number of hours for a continuous power output of 321 MW (Fig. 7a) and the maximum power output for the first 30 min (Fig. 7b) were both analysed at a permeability of 1000 mD in the storage formation. Both results show a linear increase with an increasing number of wells. A minimum of six wells was required to provide 321 MW for 6 h. If 13 wells were used, the designed CAES plant produced 321 MW of power for up to 40 h, corresponding to an electric energy production of 12 840 MWh; for the first 30 min, it produced maximally 991 MW of power. It was found that by using one additional well, the storage formation can continuously produce 321 MW of power for 4.8 h longer, and the maximum power output for the first 30 min was increased by 76 MW. Together with the deliverability analysis, this allows a rough design of the CAES storage set-up to be made.

Discussion

Using the Huntorf power plant as a reference, the two salt caverns provide a total volume of roughly 3.1×10^5 m^3 and 321 MW of power for up to 3 h (Crotogino *et al.* 2001). The corresponding storage capacity is 963 MWh and the energy density is about 3.1 kWh m^{-3}. As shown in Figure 7a, a porous formation with a permeability of 1000 mD may provide 321 MW for up to 8 h using six wells and a total volume of air in place of about 4.2×10^6 m^3. The corresponding storage capacity is 2568 MWh and the energy density is about 0.6 kWh m^{-3}. If 13 wells are used, the energy density can reach about 3.1 kWh m^{-3} and the formation has a much higher capacity of 12 840 MWh. So while CAES in salt caverns is scalable by increasing the number of caverns, porous media CAES is scalable by increasing the gas in place and the number of wells.

Compared to salt caverns, the hydraulic permeability of porous formations represents an inherent limitation on the achievable air flow rates (Kushnir *et al.* 2012*a*). The sensitivity analysis based on the average permeability performed in this work provides a first step towards estimating the number of wells needed and designing a cost-effective CAES facility. There are additional factors that influence reservoir performance, such as the anticline closure radius, the well configuration, permeability distribution and residual water saturation.

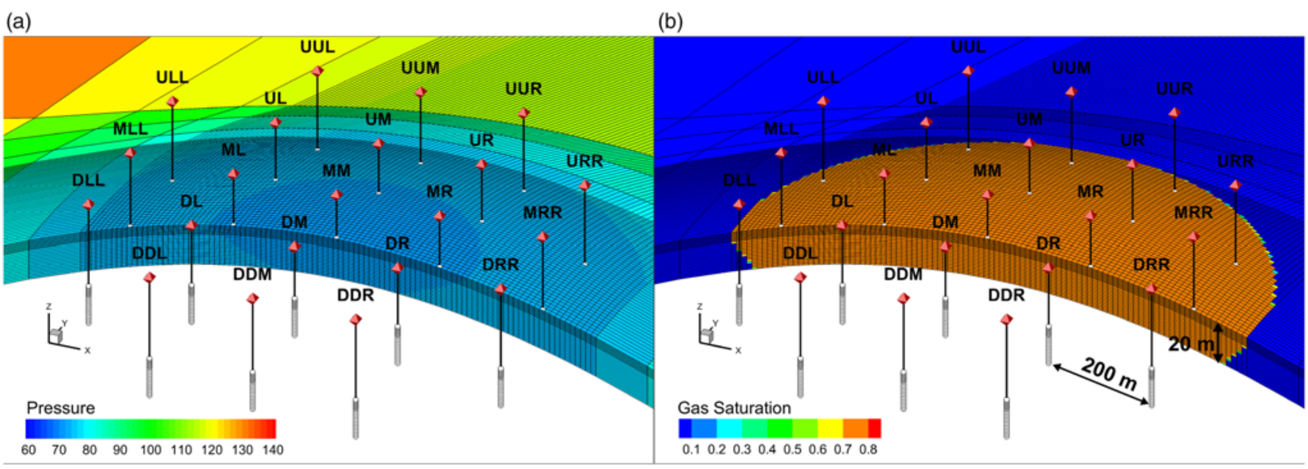

Fig. 4 Side view of an initial pressure distribution (**a**) and gas phase distribution (**b**) in the gas reservoir (using a vertical exaggeration of ×4). The spatial distribution of 21 wells within a minimum distance of 200 m is shown. For the scenario using six wells, the wells UL, ML, DL, UR, MR and DR are used.

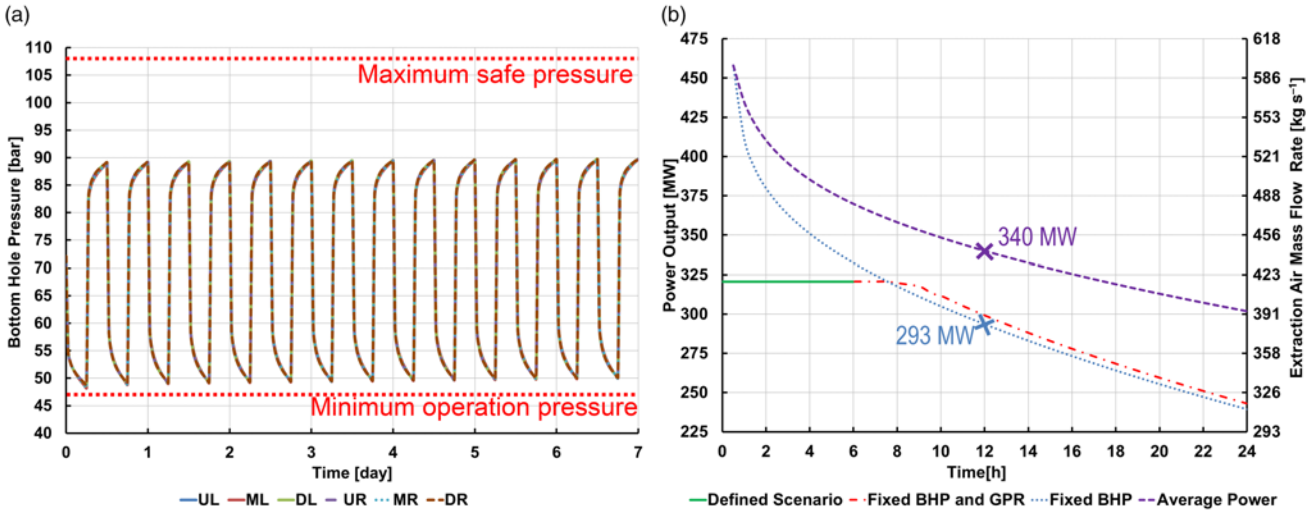

Fig. 5. (**a**) Bottom hole pressure (BHP) response of the six wells during the cyclic operation. (**b**) Extraction air mass flow rate (right axis) and power output (left axis) for: continuous power output as the designed scenario ('Defined scenario': solid line), continuous power output by fixing BHP and extraction air mass flow rate ('Fixed BHP and GPR': dash dotted line), instantaneous power output by fixing BHP ('Fixed BHP: dotted line), and average power output calculated based on the instantaneous power output ('Average power': dashed line).

The closure radius of the anticline must be at least as large as the radius of the required air volume (Succar & Williams 2008). In the scenario used in this work, the initial air volume is present within a radius of approximately 500 m, which is about one-sixth of the anticline closure radius. This large closure radius would thus allow the stored air volume to increase, which increases the storage capacity, as well as the rates, if more wells are also used. With a smaller closure radius but the same vertical drop, the dip angle of the anticline will increase. This will reduce the effect of gravity override during injection, helping the gas to aggregate at the top of the anticline and therefore enhance extraction rates due to higher gas saturations close to the wells.

Because of the variable thickness of storage formations, the well screen length (i.e. the open-hole section) needs to be adjusted to avoid water coning (Wiles & McCann 1981). The shorter the well screen length, the higher the pressure response while maintaining a required gas flow rate. When pressure is limited, however, only lower flow rates can be achieved. The larger the well distance, the less interference occurs, so that higher air flow rates can be applied. However, with increasing well distance, fewer wells can be placed within the gas reservoir, which lowers the total extraction rate from the storage site. Instead of vertical wells, horizontal wells could be used, providing a higher deliverability, especially for low-permeable storage formations.

Permeability will also vary spatially around the average value used in the sensitivity analysis in horizontal and vertical directions because of formation heterogeneity. This would be likely to lower the deliverability and thus increase the number of wells required to achieve the target rate, with the number of wells depending strongly on the type of local permeability and porosity heterogeneity. For real storage applications, well deliverability tests and history matching are applied to determine the required number of wells (Hydrodynamics Group LCC 2011). The residual water saturation was assumed to be constant at 0.2 in the sensitivity analysis. A larger residual water saturation would reduce the air volume in the pore space, and thus the available amount of air accessible to each well during injection or extraction. This may limit the time that a continuous gas extraction rate can be upheld to provide a continuous power output, especially for low-permeability formations. According to the well deliverability curves in the Pittsfield test (ANR Storage Company 1990), the air flow rates of wells will decrease if turbulent flow close to wells is encountered. This non-Darcy behaviour can lower the maximum power output within the first 30 min due to a high extraction flow rate: however, this is not considered in this work.

Apart from the reservoir performance analysis, induced impacts can be considered when assessing this energy storage option (Bauer *et al.* 2013). Because this paper focuses on the dimensioning aspects of a porous media compressed air storage, a quantitative evaluation of possible induced impacts is beyond the scope of this paper and thus a qualitative discussion is given here. The current operating CAES facilities at Huntorf and McIntosh operate as diabatic storage sites, which lose heat during compression of the air and regain this heat by burning natural gas with the compressed air during expansion. The thermal energy from the compression is not stored. According to the design of the Huntorf power plant (Crotogino *et al.* 2001), the temperature of the injected air at the well head after the compressor is cooled to the ambient temperature of the rock salt cavern. At the well bottom hole, the air temperatures may increase by a few kelvin due to the slight pressure increase along the well. The local geothermal gradient determines the ambient temperature of the reservoir formation and thus the temperature to which the air would be cooled. During air extraction, the compressed air with the ambient temperature of the geological formation will expand along the well. This temperature decrease, however, is small compared to the decrease in temperature caused by the expansion of the gas in the turbine. A higher geothermal gradient would thus be beneficial, as air does not have to be cooled so much and less natural gas is required during air expansion in the turbine. Injecting air at higher temperatures would thus also be beneficial, but the mechanical integrity of the host rock would have to be proven. Storing the compression heat for heating the expanding gas is an idea for an adiabatic CAES that is currently at the research stage (RWE Power 2010). The main problem here is the high heating rates required.

The injection of oxygen as a component of air into geological formations long free of oxygen may cause geochemical reactions. As an analogy, injection of CO_2 for CO_2 storage (CO_2 capture and storage (CCS)) with about 4% of O_2 as an impurity may lead to mineral oxidation if redox-sensitive minerals or ferrous iron-bearing minerals are present in the storage formation. This is especially so in the case of pyrite (Lu *et al.* 2014; André *et al.* 2015). Pyrite oxidation increases the dissolution of carbonates, as these buffer the H^+ from pyrite dissolution, typically leading to gypsum precipitates. This reaction was found to stop once the oxygen is consumed. During operation of CAES, oxygen is injected into the storage formation with each injection cycle, which could result in a lower

Table 3. *A list of the varied permeabilities and porosities in the sensitivity analysis*

Parameter	Storage formation													
Permeability [mD]	10	100	200	300	400	500	600	700	800	900	1000	1500	2000	2500
Porosity [−]	0.15	0.25	0.25	0.30	0.30	0.30	0.30	0.30	0.35	0.35	0.35	0.40	0.40	0.40

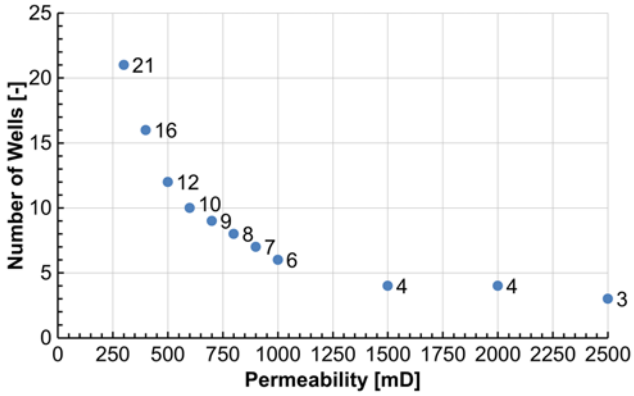

Fig. 6. Number of wells needed to support the defined CAES scenario v. permeability of the storage formation.

pH of the storage formation water and thus a higher risk of wellbore corrosion, as well as a reduced oxygen content in the outflowing air. Precipitates, such as ferrous sulphate or gypsum, in the storage formation might reduce porosity, and thus also permeability and well deliverability (Succar & Williams 2008). However, research by Huminicki & Rimstidt (2009) and Berta *et al.* (2016) has shown that if enough carbonates are present in the mineral phases or dissolved in the fluid phase, the pH of the formation water will remain at neutral levels. Ferric-ion-containing hydroxide was found to precipitate mainly on the pyrite mineral surfaces, and therefore forms a coating that strongly limits further pyrite oxidation and thus oxygen consumption. These geochemical impacts thus depend on the chemical composition of the storage formation and the formation water, but can be experimentally assessed using site-specific data.

In the Huntorf power plant, due to the high-pressure reduction rates (up to 15 bar h^{-1}), the stability of the surrounding salt and the volume losses have been monitored over its life period (Crotogino *et al.* 2001). The corrosion of production strings has been discovered in the Huntorf power plant because of the humidity of the air. In porous formation CAES, the same risks should be considered, as well as potential brine movement or uprising induced by large-scale pressure built-up due to the initial fill (e.g. see Delfs *et al.* 2016). The production string can have a higher risk of corrosion due to the presence of residual water and the possible production of acid due to mineral oxidation. While for a salt cavern the spatial position is known exactly, the spatial position of the gas phase for a porous formation CAES is not. However, geophysical monitoring techniques, such as seismic, geoelectric and gravimetric measurements, might be employed to monitor the extension of the gas phase (Benisch *et al.* 2015; al Hagrey *et al.* 2016; Köhn *et al.* 2016; Pfeiffer *et al.* 2016).

Summary and outlook

A hypothetical scenario of large-scale CAES operation using a porous formation as the storage site was numerically simulated within a typical geological anticline structure in northern Germany. During the cyclic operation, the pressure fluctuation in the reservoir was found to be within the system thresholds, thus supporting the

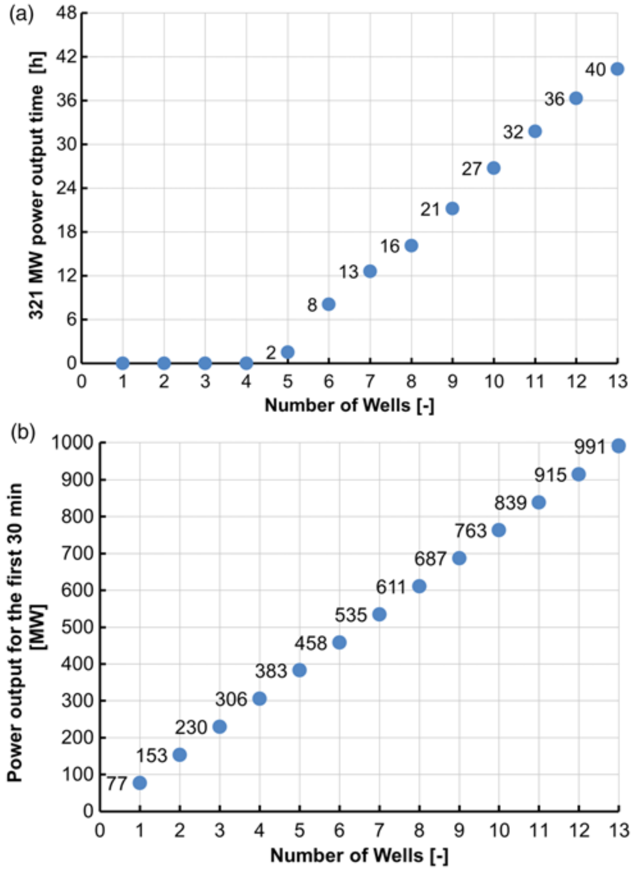

Fig. 7. Hours of continuous power output (**a**) and the maximum short-term power output (**b**) provided for different numbers of wells used (at a permeability of 1000 mD).

specified injection and extraction air mass flow rates of 430 kg s^{-1} and 417 kg s^{-1}, respectively. This shows that it is feasible to operate the designed CAES scenario using this porous formation. Using six injection and extraction wells, 321 MW of power could be produced from the stored air for 6 h, corresponding to an energy production of 1926 MWh. A deliverability analysis shows that the reservoir can continuously support 321 MW of power production for up to 8 h before reaching the minimum operating pressure, thereby extracting about 3.5% of the total air in the reservoir. Furthermore, for the first 30 min, the maximum achievable extraction air mass rate of the storage formation is higher at 596 kg s^{-1}, corresponding to 458 MW of power. Instantaneous power output dropped from 458 to 293 MW within the first 12 h.

The number of wells required was estimated accounting for different permeabilities of the storage formation. When the permeability was less than 300 mD, the storage formation was not able to deliver the specified extraction air mass flow rate for 6 h, even when 21 wells were used. A minimum of three wells was always required, even for a permeability of 2500 mD, and well interference has also to be considered. For each additional well, the storage formation can continuously produce the required power of 321 MW for 4.8 h longer; while for the first 30 min, the maximum power output is increased by 76 MW. The combination of the deliverability analysis, which also covers shorter time periods, and the analysis of the number of wells required at different permeabilities allows a first design of such a CAES storage site in a permeable porous formation to be made.

However, there are many other possible aspects to be considered for such a CAES storage facility, as discussed above, such that this study can provide only a first step towards such a design. A study investigating different well configurations, and combinations of horizontal and vertical wells, will allow for an optimized utilization of a chosen anticline site (Mitiku & Bauer 2013). A site-specific heterogeneity study based on stratigraphic facies modelling could provide a statistical estimation of the range of possible power output rates for the CAES applications. A similar study for hydrogen porous media storage was performed by Pfeiffer *et al.* (2017). Methodology and simulation codes by Beyer *et al.* (2012), Mitiku *et al.* (2013) and, especially, Li *et al.* (2014), who coupled a geochemical simulator to the ECLIPSE reservoir simulation software, can be used to estimate the potential changes in permeability due to chemical reactions, including porosity and permeability feedbacks.

Acknowledgements The presented work is part of the ANGUS+ research project (www.angusplus.de). We gratefully acknowledge the support of Project Management Jülich (PTJ). Also, we thank Wolf Tilmann Pfeiffer for all his great help and fruitful discussions.

Funding We gratefully acknowledge the funding of the ANGUS+ joint project by the German Federal Ministry of Education and Research (BMBF) under the grant number of 03EK3022 as part of the Energy Storage Funding Initiative 'EnergieSpeicher' of the German Federal Government.

References

al Hagrey, S.A., Schäfer, D., Köhn, D., Wiegers, C.E., Chung, D., Dahmke, A. & Rabbel, W. 2016. Monitoring gas leakages simulated in a near surface aquifer of the Ellerbek paleo-channel. *Environmental Earth Sciences*, **75**, 1083, https://doi.org/10.1007/s12665-016-5784-1

André, L., Azaroual, M., Bernstone, C. & Wittek, A. 2015. Modeling the geochemical impact of an injection of CO_2 and associated reactive impurities (SO_2 and O_2) into a saline reservoir. *Transport in Porous Media*, **108**, 185–205, https://doi.org/10.1007/s11242-014-0359-7

ANR Storage Company. 1990. *Compressed-Air Energy Storage: Pittsfield Aquifer Field Test; Test Data: Engineering Analysis and Evaluation*. ANR Storage Company, Detroit, MI, USA.

Baldschuhn, R., Binot, F., Fleig, S. & Kockel, F. 2001. *Geotektonischer Atlas von Nordwest-Deutschland und dem deutschen Nordsee-Sektor* [Tectonic Atlas of Northwest Germany and the German North Sea Sector]. Schweizerbart Science Publishers, Stuttgart, Germany.

Bary, A., Crotogino, F. *et al*. 2002. Storing natural gas underground. *Oilfield Review*, **14**, 16.

Bauer, S., Beyer, C. *et al*. 2013. Impacts of the use of the geological subsurface for energy storage: An investigation concept. *Environmental Earth Sciences*, **70**, 3935–3943, https://doi.org/10.1007/s12665-013-2883-0

Benisch, K. & Bauer, S. 2013. Short- and long-term regional pressure build-up during CO_2 injection and its applicability for site monitoring. *International Journal of Greenhouse Gas Control*, **19**, 220–233, https://doi.org/10.1016/j.ijggc.2013.09.002

Benisch, K., Köhn, D., al Hagrey, S., Rabbel, W. & Bauer, S. 2015. A combined seismic and geoelectrical monitoring approach for CO_2 storage using a synthetic field site. *Environmental Earth Sciences*, **73**, 3077–3094, https://doi.org/10.1007/s12665-014-3603-0

Berta, M., Dethlefsen, F., Ebert, M., Gundske, K. & Dahmke, A. 2016. Surface passivation model explains pyrite oxidation kinetics in column experiments with up to 11 bars $p(O_2)$. *Environmental Earth Sciences*, **75**, 1175, https://doi.org/10.1007/s12665-016-5985-7

Beyer, C., Li, D., De Lucia, M., Kühn, M. & Bauer, S. 2012. Modelling CO_2-induced fluid–rock interactions in the Altensalzwedel gas reservoir. Part II: coupled reactive transport simulation. *Environmental Earth Sciences*, **67**, 573–588, https://doi.org/10.1007/s12665-012-1684-1

BMWi. 2015. *Making a Success of the Energy Transition*. Federal Ministry for Economic Affairs and Energy (BMWi), Berlin, Germany.

Bockmeyer, A. & Bauer, S. 2016. Efficient simulation of multiple borehole heat exchanger storage sites. *Environmental Earth Sciences*, **75**, 1021, https://doi.org/10.1007/s12665-016-5773-4

Brooks, R. & Corey, A. 1964. *Hydraulic Properties of Porous media*. Hydrology Papers, Colorado State University, **3**.

Bundesnetzagentur. 2015. *Monitoringbericht* [Monitoring Report]. Bundesnetzagentur für Elektrizität, Gas Telekommunikation, Post und Eisenbahnen, Bonn, Germany.

Çengel, Y.A. & Boles, M.A. 2011. *Thermodynamics: An Engineering Approach*. 7th edn. McGraw-Hill, Boston, MA, USA.

Crotogino, F., Mohmeyer, K.-U. & Scharf, R. 2001. Huntorf CAES: More than 20 years of successful operation. *In*: Proceedings of the Solution Mining Research Institute (SMRI) Spring Meeting, Orlando, FL, USA, 15–18 April 2001. Solution Mining Research Institute (SMRI), Clarks Summit, PA, USA, 351–357.

Delfs, J.-O., Nordbeck, J. & Bauer, S. 2016. Upward brine migration resulting from pressure increases in a layered subsurface system. *Environmental Earth Sciences*, **75**, 1441, https://doi.org/10.1007/s12665-016-6245-6

Dethlefsen, F., Ebert, M. & Dahmke, A. 2014. A geological database for parameterization in numerical modeling of subsurface storage in northern Germany. *Environmental Earth Sciences*, **71**, 2227–2244, https://doi.org/10.1007/s12665-013-2627-1

E.ON SE. 2016. Kraftwerk Huntorf, http://www.eon.com/de/ueber-uns/struktur/asset-finder/huntorf-power-station.html

European Commission. 2015. *Renewable Energy Progress Report*. European Commission, Brussels, Belgium.

Goudar, C. & Sonnad, J. 2008. Comparison of the iterative approximations of the Colebrook–White equation. *Hydrocarbon Processing*, **87**, (8), 79–80, 83.

Hagoort, J. 1988. *Fundamentals of Gas Reservoir Engineering*. Elsevier Science, Amsterdam, The Netherlands.

Hartmann, N., Vöhringer, O., Kruck, C. & Eltrop, L. 2012. Simulation and analysis of different adiabatic Compressed Air Energy Storage plant configurations. *Applied Energy*, **93**, 541–548, https://doi.org/10.1016/j.apenergy.2011.12.007

Hese, F. 2011. Geologische 3D-Modelle des Untergrundes Schleswig-Holsteins – ein Beitrag für Potenzialstudien zur Nutzung von tiefen salinen Aquiferen [Geological 3D models of the subsurface of Schleswig-Holstein – a contribution to studies focused on the utilisation potential of deep saline aquifers]. *Zeitschrift der Deutschen Gesellschaft für Geowissenschaften*, **162**, 389–404, https://doi.org/10.1127/1860-1804/2011/0162-0389

Hese, F. 2012. *3D Modellierungen und Visualisierung von Untergrundstrukturen für die Nutzung des unterirdischen Raumes in Schleswig-Holstein* [3D Modelling and Visualization of Subsurface Structures for the Use of the Subsurface Space of Schleswig-Holstein]. PhD thesis, University of Kiel, Kiel, Germany.

Heusermann, S., Rolfs, O. & Schmidt, U. 2003. Nonlinear finite-element analysis of solution mined storage caverns in rock salt using the LUBBY2 constitutive model. *Computers and Structures*, **81**, 629–638, https://doi.org/10.1016/S0045-7949(02)00415-7

Hoffeins, H. 1994. *Huntorf Air Storage Gas Turbine Power Plant. Energy Supply*. Brown Boveri & Cie Publications, D GK 90 202 E.

Hoffeins, H. & Mohmeyer, K.-U. 1986. Operating experience with the Huntorf air-storage gas turbine power station. *Brown Boveri Review*, **73**, 297–305.

Huminicki, D.M.C. & Rimstidt, J.D. 2009. Iron oxyhydroxide coating of pyrite for acid mine drainage control. *Applied Geochemistry*, **24**, 1626–1634, https://doi.org/10.1016/j.apgeochem.2009.04.032

Hydrodynamics Group LCC. 2011. *Iowa Stored Energy Plant Agency Compressed-Air Energy Storage Project: Final Project Report – Dallas Center Mt. Simon Structure CAES System Performance Analysis*. Report Prepared for Iowa Storage Energy Plant Agency, Des Moines, IA, USA.

Ibrahim, H., Younès, R., Ilinca, A., Dimitrova, M. & Perron, J. 2010. Study and design of a hybrid wind-diesel-compressed air energy storage system for remote areas. *Applied Energy*, **87**, 1749–1762, https://doi.org/10.1016/j.apenergy.2009.10.017

IPCC. 2014. *Climate Change 2014: Mitigation of Climate Change*. Intergovernmental Panel on Climate Change (IPCC), Geneva, Switzerland. Cambridge University Press, Cambridge, https://doi.org/10.1017/CBO9781107415416

Kabuth, A., Dahmke, A. *et al*. 2017. Energy storage in the geological subsurface: dimensioning, risk analysis and spatial planning: the ANGUS+ project. *Environmental Earth Sciences*, **76**, 23, https://doi.org/10.1007/s12665-016-6319-5

Kaye, G.W.C. & Laby, T.H. 2016. 3.5. Critical constants and second virial coefficients of gases. *In: Tables of Physical and Chemical Constants*. 16th edn. Kaye & Laby Online, www.kayelaby.npl.co.uk

Kepplinger, J., Crotogino, F., Donadei, S. & Wohlers, M. 2011. Present trends in compressed air energy and hydrogen storage in Germany. *In*: Proceedings of the Solution Mining Research Institute (SMRI) Fall 2011 Technical Conference, York, United Kingdom, 3–4 October 2011. Solution Mining Research Institute (SMRI), Clarks Summit, PA, USA, 1–12.

Khaledi, K., Mahmoudi, E., Datcheva, M., König, D. & Schanz, T. 2016*a*. Sensitivity analysis and parameter identification of a time dependent constitutive model for rock salt. *Journal of Computational and Applied Mathematics*, **293**, 128–138, https://doi.org/10.1016/j.cam.2015.03.049

Khaledi, K., Mahmoudi, E., Datcheva, M. & Schanz, T. 2016*b*. Analysis of compressed air storage caverns in rock salt considering thermo-mechanical cyclic loading. *Environmental Earth Sciences*, **75**, 1149, https://doi.org/10.1007/s12665-016-5970-1

Kim, Y.M., Shin, D.G. & Favrat, D. 2011. Operating characteristics of constant-pressure compressed air energy storage (CAES) system combined with pumped hydro storage based on energy and exergy analysis. *Energy*, **36**, 6220–6233, https://doi.org/10.1016/j.energy.2011.07.040

Kim, Y.M., Lee, J.H., Kim, S.J. & Favrat, D. 2012. Potential and evolution of compressed air energy storage: Energy and exergy analyses. *Entropy*, **14**, 1501–1521, https://doi.org/10.3390/e14081501

Klaus, T., Vollmer, C., Werner, K., Lehmann, H. & Müschen, K. (eds). 2010. *Energy Target 2050: 100% Renewable Electricity Supply*. Umweltbundesamt, Dessau-Roßlau, Germany.

Köhn, D., De Nil, D., al Hagrey, S.A. & Rabbel, W. 2016. A combination of waveform inversion and reverse-time modelling for microseismic event characterization in complex salt structures. *Environmental Earth Sciences*, **75**, 1235, https://doi.org/10.1007/s12665-016-6032-4

Kushnir, R., Ullmann, A. & Dayan, A. 2010. Compressed air flow within aquifer reservoirs of CAES plants. *Transport in Porous Media*, **81**, 219–240, https://doi.org/10.1007/s11242-009-9397-y

Kushnir, R., Dayan, A. & Ullmann, A. 2012*a*. Temperature and pressure variations within compressed air energy storage caverns. *International Journal of Heat and Mass Transfer*, **55**, 5616–5630, https://doi.org/10.1016/j.ijheatmasstransfer.2012.05.055

Kushnir, R., Ullmann, A. & Dayan, A. 2012*b*. Thermodynamic and hydrodynamic response of compressed air energy storage reservoirs: A review. *Reviews in Chemical Engineering*, **28**, 123–148, https://doi.org/10.1515/revce-2012-0006

LBEG. 2015. Untertage-Gasspeicherung in Deutschland [Underground Gas Storage in Germany]. *Erdöl Erdgas Kohle,* **131**, 398–406.

Lemmon, E.W., Jacobsen, R.T., Penoncello, S.G. & Firend, D.G. 2000. Thermodynamic properties of air and mixtures of nitrogen, argon, and oxygen from 60 to 2000K at pressures to 2000MPa. *Journal of Physical and Chemical Reference Data*, **29**, 331–385, https://doi.org/10.1063/1.1285884

Li, D., Bauer, S., Benisch, K., Graupner, B. & Beyer, C. 2014. OpenGeoSys-ChemApp: A coupled simulator for reactive transport in multiphase systems and application to CO_2 storage formation in Northern Germany. *Acta Geotechnica*, **9**, 67–79, https://doi.org/10.1007/s11440-013-0234-7

Lu, J., Mickler, P.J., Nicot, J.-P., Yang, C. & Romanak, K.D. 2014. Geochemical impact of oxygen on siliciclastic carbon storage reservoirs. *International Journal of Greenhouse Gas Control*, **21**, 214–231, https://doi.org/10.1016/j.ijggc.2013.12.017

Luo, X., Wang, J. *et al*. 2016. Modelling study, efficiency analysis and optimisation of large-scale Adiabatic Compressed Air Energy Storage systems with low-temperature thermal storage. *Applied Energy*, **162**, 589–600, https://doi.org/10.1016/j.apenergy.2015.10.091

MELUR. 2015. *Abregelung von Strom aus erneuerbaren Energien und daraus resultierende Entschädigungsansprüche in den Jahren 2010 bis 2014* [Curtailment of Renewable Power Production and Resulting Compensation Claims in the Years 2010 to 2014]. Ministerium für Energiewende, Landwirtschaft, Umwelt und ländliche Räume Schleswig-Holstein (MELUR), Kiel, Germany.

Mitiku, A.B. & Bauer, S. 2013. Optimal use of a dome-shaped anticline structure for CO_2 storage: a case study in the North German sedimentary basin. *Environmental Earth Sciences*, **70**, 3661–3673, https://doi.org/10.1007/s12665-013-2580-z

Mitiku, A.B., Li, D., Bauer, S. & Beyer, C. 2013. Geochemical modelling of CO_2–water–rock interactions in a potential storage formation of the North German sedimentary basin. *Applied Geochemistry*, **36**, 168–186, https://doi.org/10.1016/j.apgeochem.2013.06.008

Morris, C. & Pehnt, M. 2012. *Energy Transition: The German Energiewende*. Heinrich Böll Stiftung , Berlin, Germany.

Nakhamkin, M., Schainker, R.B., Chiruvolu, M., Patel, M., Byrd, S. & Marean, J. 2009. Second generation of CAES technology – performance, operations, economics, renewable load management, green energy. Paper presented at POWER-GEN International, 8–10 December 2009, Las Vegas, Nevada, USA.

Nazary Moghadam, S., Mirzabozorg, H. & Noorzad, A. 2013. Modeling time-dependent behavior of gas caverns in rock salt considering creep, dilatancy and failure. *Tunnelling and Underground Space Technology*, **33**, 171–185, https://doi.org/10.1016/j.tust.2012.10.001

Oldenburg, C.M. & Pan, L. 2013*a*. Porous media compressed-air energy storage (PM-CAES): Theory and simulation of the coupled wellbore–reservoir system. *Transport in Porous Media*, **97**, 201–221, https://doi.org/10.1007/s11242-012-0118-6

Oldenburg, C.M. & Pan, L. 2013*b*. Utilization of CO_2 as cushion gas for porous media compressed air energy storage. *Greenhouse Gases: Science and Technology*, **3**, 124–135, https://doi.org/10.1002/ghg.1332

Pei, P., Korom, S.F., Ling, K., He, J. & Gil, A. 2015. Thermodynamic impact of aquifer permeability on the performance of a compressed air energy storage plant. *Energy Conversion and Management*, **97**, 340–350, https://doi.org/10.1016/j.enconman.2015.03.072

Pfeiffer, W.T. & Bauer, S. 2015. Subsurface porous media hydrogen storage – scenario development and simulation. *Energy Procedia*, **76**, 565–572, https://doi.org/10.1016/j.egypro.2015.07.872

Pfeiffer, W.T., al Hagrey, S.A., Köhn, D., Rabbel, W. & Bauer, S. 2016. Porous media hydrogen storage at a synthetic, heterogeneous field site: numerical simulation of storage operation and geophysical monitoring. *Environmental Earth Sciences*, **75**, 1177, https://doi.org/10.1007/s12665-016-5958-x

Pfeiffer, W.T., Beyer, C. & Bauer, S. 2017. Hydrogen storage in a heterogeneous sandstone formation: dimensioning and induced hydraulic effects. *Petroleum Geoscience*. First published online March 9, 2017, https://doi.org/10.1144/petgeo2016-050

Popp, S., Beyer, C., Dahmke, A., Koproch, N., Köber, R. & Bauer, S. 2016. Temperature-dependent dissolution of residual non-aqueous phase liquids: model development and verification. *Environmental Earth Sciences*, **75**, 953, https://doi.org/10.1007/s12665-016-5743-x

Raju, M. & Khaitan, S.K. 2012. Modeling and simulation of compressed air storage in caverns: A case study of the Huntorf plant. *Applied Energy*, **89**, 474–481, https://doi.org/10.1016/j.apenergy.2011.08.019

Reitenbach, V., Ganzer, L., Albrecht, D. & Hagemann, B. 2015. Influence of added hydrogen on underground gas storage: a review of key issues. *Environmental Earth Sciences*, 6927–6937, https://doi.org/10.1007/s12665-015-4176-2

RWE Power. 2010. *ADELE – Adiabatic Compressed-Air Energy Storage for Electricity Supply*. RWE Power, Essen, Germany, http://www.rwe.com/web/cms/mediablob/en/391748/data/364260/1/rwe-power-ag/innovations/Brochure-ADELE.pdf

Schlumberger. 2016. *Eclipse Reservoir Simulation Software v 2016.1 – Technical Description Manual*. Schlumberger Ltd, Houston, TX, USA.

Schulte, R.H., Critelli, N., Holst, K. & Huff, G. 2012. *Lessons from Iowa: Development of a 270 Megawatt Compressed Air Energy Storage Project in Midwest Independent System Operator*. Sandia Report SAND2012-0388. Sandia National Laboratories, Albuquerque, NM/ Livermore, CA, USA.

Sternberg, A. & Bardow, A. 2015. Power-to-What? – Environmental assessment of energy storage systems. *Energy & Environmental Science*, **8**, 389–400, https://doi.org/10.1039/C4EE03051F

Sterner, M. & Stadler, I. 2014. *Energiespeicher – Bedarf, Technologien, Integration* [Energy Storage – Demand, Technology, Integration]. Springer, Berlin, https://doi.org/10.1007/978-3-642-37380-0

Succar, S. & Williams, R. 2008. *Compressed Air Energy Storage: Theory, Resources, and Applications for Wind Power*. Princeton University, Energy Analysis Group, Princeton, NJ, USA.

Wiles, L.E. & McCann, R.A. 1981. *Water Coning in Porous Media Reservoirs for Compressed Air Energy Storage*. Technical Report PNL-3047. Pacific Northwest Laboratory, Richland, WA, USA.